doi:10.1093/plphys/kiab114 PLANT PHYSIOLOGY 2021: 186: 998–1012

Plant Physiology®

Research Article

The impact of slow stomatal kinetics on photosynthesis and water use efficiency under fluctuating light

David Eyland [1], Jelle van Wesemael,[1] Tracy Lawson [2] and Sebastien Carpentier [1,3,*,†]

1 Division of Crop Biotechnics, Laboratory of Tropical Crop Improvement, KU Leuven, Leuven, Belgium
2 School of Life Sciences, University of Essex, Colchester, Essex, UK
3 Bioversity International, Banana Genetic Resources, Leuven, Belgium

*Author for communication: s.carpentier@cgiar.org
†Senior author.

S.C. and T.L. supervised the experiments. D.E. performed the leaf gas exchange experiments. J.v.W. performed the whole-plant transpiration experiment. D.E., J.v.W., and S.C. analyzed the data. D.E., T.L., and S.C. wrote the manuscript. All authors reviewed and approved the final manuscript.
The author responsible for distribution of materials integral to the findings presented in this article in accordance with the policy described in the Instructions for Authors (https://academic.oup.com/plphys/pages/general-instructions) is: Sebastien Carpentier (s.carpentier@cgiar.org).

Abstract

Dynamic light conditions require continuous adjustments of stomatal aperture. The kinetics of stomatal conductance (g_s) is hypothesized to be key to plant productivity and water use efficiency (WUE). Using step-changes in light intensity, we studied the diversity of light-induced g_s kinetics in relation to stomatal anatomy in five banana genotypes (*Musa* spp.) and modeled the impact of both diffusional and biochemical limitations on photosynthesis (A). The dominant A limiting factor was the diffusional limitation associated with g_s kinetics. All genotypes exhibited a strong limitation of A by g_s, indicating a priority for water saving. Moreover, significant genotypic differences in g_s kinetics and g_s limitations of A were observed. For two contrasting genotypes, the impact of differential g_s kinetics was further investigated under realistic diurnally fluctuating light conditions and at the whole-plant level. Genotype-specific stomatal kinetics observed at the leaf level was corroborated at whole-plant level by transpiration dynamics, validating that genotype-specific responses are still maintained despite differences in g_s control at different locations in the leaf and across leaves. However, under diurnally fluctuating light conditions the impact of g_s speediness on A and intrinsic ($_i$WUE) depended on time of day. During the afternoon there was a setback in kinetics: absolute g_s and g_s responses to light were damped, strongly limiting A and impacting diurnal $_i$WUE. We conclude the impact of differential g_s kinetics depended on target light intensity, magnitude of change, g_s prior to the change in light intensity, and particularly time of day.

Introduction

In order to survive, plants need to balance CO_2 uptake for photosynthesis (A) with water loss via transpiration. By adjusting their aperture, stomata control gaseous exchange between the leaf interior, and the external atmosphere. Stomatal aperture is adjusted by moving solutes into or out of the guard cells. These changes in osmotic potential elicit water movement in or out of the guard cells, altering turgor pressure and subsequently aperture. In general, stomatal opening in well-watered C3 and C4 species is triggered by high light intensity, low vapor pressure deficit (VPD), and low CO_2 concentrations. Opposite environmental conditions

Received November 13, 2020. Accepted February 23, 2021. Advance access publication March 8, 2021

Open Access

(low light, high VPD, and high CO_2) stimulate stomatal closure (Assmann and Shimazaki, 1999; Outlaw, 2003; Lawson and Morison, 2004). Therefore, in a dynamic field environment, stomata are continuously adjusting the aperture to achieve an appropriate balance between carbon gain and water loss (Pearcy, 1990; Lawson and Blatt, 2014). Most research has studied stomatal conductance (g_s) and A under steady-state conditions. A high g_s under steady-state conditions is associated with high A and consequently improved growth (Fischer et al., 1998; Franks, 2006). However, as g_s kinetics are typically a magnitude slower than those of A, the speed at which these steady-state values are reached in a fluctuating environment have a great influence on the growth and water use efficiency (WUE; Lawson and Blatt, 2014; Kaiser et al., 2016; McAusland et al., 2016; Taylor and Long, 2017; De Souza et al., 2020; Yamori et al., 2020). In a fluctuating field environment, light intensity is one of the most variable environmental conditions as it changes continuously by moving cloud covers and shading from adjacent plants (Pearcy, 1990; Slattery et al., 2018; Morales and Kaiser, 2020). In this way, stomata frequently experience alternating light intensities, inducing stomatal responses that change A, g_s, and the ratio of these, the intrinsic WUE ($_i$WUE). The balance between CO_2 gain and H_2O loss under changing light intensities is disturbed by delayed g_s responses (Vialet-Chabrand et al., 2017; Slattery et al., 2018). Limitations of A after an increase in light intensity are the combination of diffusional and biochemical limitations. Biochemical activation has been shown to majorly limit A during short light flecks (Soleh et al., 2017; Taylor and Long, 2017; Acevedo-Siaca et al., 2020). Under longer light periods, limitations have been mainly attributed to stomatal limitations, with biochemical activation only limiting for a short time (<10 min) because of rapid activation of RuBP regeneration and Rubisco (Mott and Woodrow, 2000; Kaiser et al., 2016; Deans et al., 2019a; De Souza et al., 2020). The slower g_s increase to increased light intensity limits the CO_2 uptake for A, while the slower g_s decrease to decreased light intensity results in unnecessary water loss. The limitation of A by the slower kinetics of g_s has been shown to be significant in well-watered C3 species (Farquhar and Sharkey, 1982; Jones, 1998; Lawson and Blatt, 2014; McAusland et al., 2016; Deans et al., 2019a). Rapid g_s kinetics, therefore, have been hypothesized to maximize A and $_i$WUE, as steady-state values under the new conditions can be rapidly achieved (Lawson and Blatt, 2014; Papanatsiou et al., 2019; De Souza et al., 2020; Kimura et al., 2020). The g_s kinetics are, together with the final steady-state g_s the plant reaches, crucial to determine the plant performance (Franks and Farquhar, 2007; Vico et al., 2011; McAusland et al., 2016; Qu et al., 2016; Faralli et al., 2019b; Yamori et al., 2020). The importance of diversity in g_s kinetics was highlighted by De Souza et al. (2020), who showed a three-fold higher variability in carbon assimilation between cassava genotypes under fluctuating light than under steady-state conditions, mainly caused by differences in stomatal limitation. However, to our knowledge, the diversity of g_s kinetics across varieties has neither been investigated at whole-plant level nor under diurnally fluctuating light conditions.

Here our research aimed to explore biodiversity in light-induced stomatal dynamics across genotypes and evaluate for the first time the impact on whole-plant level. We studied the diversity of light-induced g_s kinetics in relation to stomatal anatomy in five banana genotypes (*Musa* spp.) with distinct transpiration phenotypes (van Wesemael et al., 2019). We modeled the impact of diffusional and biochemical kinetics on A under single step-changes in light intensity and modeled the impact of differential g_s kinetics on A and $_i$WUE under realistic diurnal fluctuating light conditions. By comparing the g_s kinetics in response to step-changes with the g_s responses under fluctuating light conditions, we gain insight into the importance of stomatal kinetics on diurnal carbon gain and WUE.

Results

A and g_s response to step changes

Increasing light intensity from 100 to 1,000 μmol m^{-2} s^{-1} induced a strong stomatal opening response (Figure 1). The g_s response followed a sigmoidal pattern. A similar sigmoidal limiting pattern was observed for A in all genotypes, indicating a strong limitation of A by g_s in banana (Figure 1). Between genotypes, there were significant differences in the speed of g_s increase. Steady-state A and g_s under high light intensity were reached in three out of five genotypes. In contrast, the genotypes Cachaco and Leite continued to increase g_s and A slowly after 90 min of 1,000 μmol m^{-2} s^{-1}. The subsequent decrease in light intensity from 1,000 to 100 μmol m^{-2} s^{-1} resulted in a rapid g_s decrease, which also followed a sigmoidal pattern (Figure 1). Photosynthesis, on the other hand, as expected decreased instantly because light became the limiting factor (Figure 1).

Modeling steady-state and light-induced responses of g_s

The steady-state g_s at 100 μmol m^{-2} s^{-1} ($g_{s,100}$) and 1,000 μmol m^{-2} s^{-1} ($g_{s,1,000}$) did not differ significantly between genotypes (Figure 2A; Supplemental Table S1). $g_{s,100}$ ranged from 0.023 to 0.040 mol $m^{-2}s^{-1}$, while $g_{s,1,000}$ ranged between 0.14 and 0.16 mol $m^{-2}s^{-1}$ (Figure 2A; Supplemental Table S1).

The speed of g_s increase varied strongly between the banana genotypes and the modeled variables differed significantly (Figure 2, B and C; Supplemental Table S1). The genotype with the slowest g_s increase, Cachaco, had an average time constant K_i of 17 min, while the fastest genotype, Mbwazirume, had a K_i of 6.4 min (Figure 2B; Supplemental Table S1). The speed of the decrease in g_s (K_d) was also genotype-dependent (Figure 2C; Supplemental Table S1). K_d was about two-fold higher in Cachaco (9.5 min) than in Mbwazirume (4.4 min). Across all genotypes, K_i was significantly correlated with K_d ($R^2 = 0.41$, $P < 0.001$; Figure 2D; Supplemental Figure S1). However, the decrease in g_s was significantly faster than the increase ($P < 0.001$). K_i was significantly correlated with the time to reach 95%, 90%, and

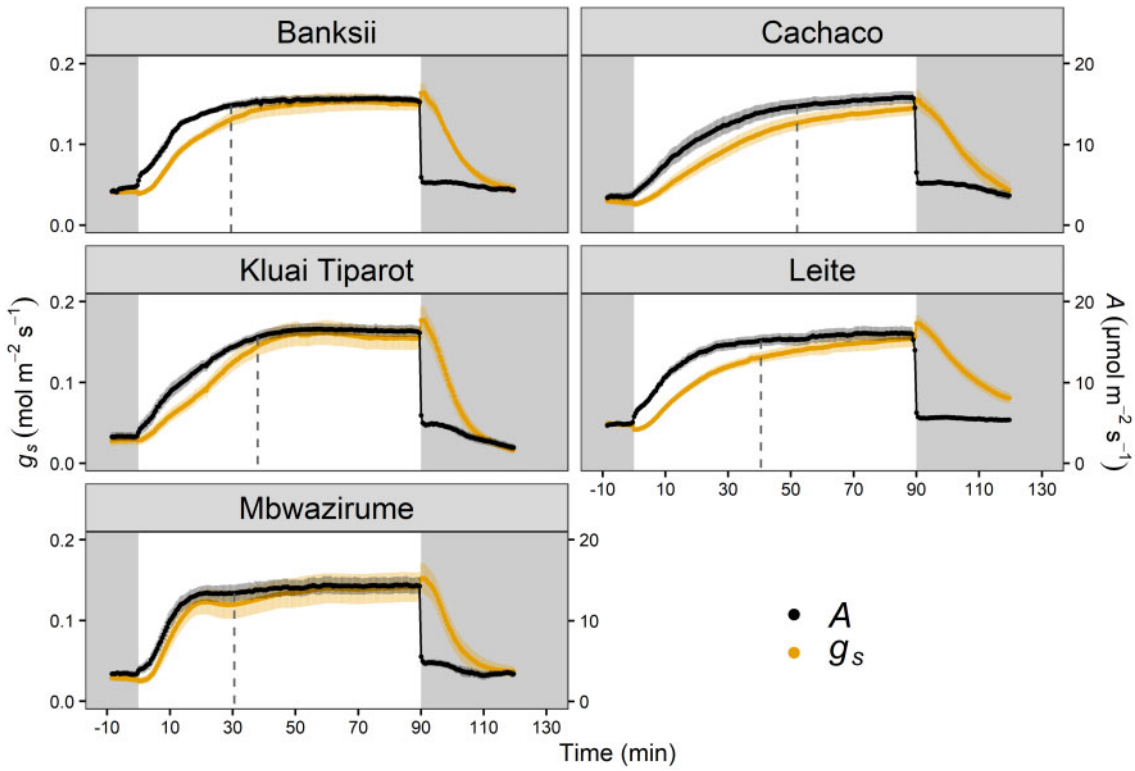

Figure 1 Response of g_s (orange) and A (black) of five banana genotypes to a step increase in light intensity from 100 to 1,000 µmol m^{-2}s^{-1} followed by a decrease from 1,000 to 100 µmol m^{-2}s^{-1}. Grey and white areas indicate time periods of 100 µmol m^{-2} s^{-1} and 1,000 µmol m^{-2}s^{-1}, respectively. Dashed lines indicate when 95% of steady-state A was reached. Points and error bars represent mean ± SE (n = 7–8).

50% of steady-state g_s under the high light intensity (R^2 = 0.27–0.57, $P < 0.001$; Supplemental Figure S1). Also the maximal slope of g_s increase and decrease ($SI_{max,i}$ and $SI_{max,d}$) were significantly correlated with the time constant K as the magnitude of g_s change was similar across genotypes (R^2 = 0.52 and 0.49 for g_s increase and decrease, respectively, $P < 0.001$; Supplemental Figure S1). During light-induced stomatal opening comparable differences across genotypes were present in $SI_{max,i}$ as in K_i. The lowest $SI_{max,i}$ values were observed for the genotype Cachaco and the highest values for Mbwazirume (Supplemental Figure S2 and Supplemental Table S1). $SI_{max,d}$ was highest for the genotype Kluai Tiparot, while Leite showed the lowest $SI_{max,d}$ (Supplemental Figure S2 and Supplemental Table S1). Analogous to the opening and closing time constant, the absolute slope of closing was significantly higher than the opening slope ($P < 0.001$).

Impact of stomatal opening speed on A

The speed of the increase in g_s following a step-change in light intensity from 100 to 1,000 µmol m^{-2} s^{-1} strongly determined CO_2 uptake during this period. The speed of changes in g_s in all genotypes accounted for >89% of A limitation (Supplemental Figure S3A). The time to reach 95% of steady-state A at 1,000 µmol m^{-2} s^{-1} ($A_{1,000}$) was >30 min for almost all genotypes and differed significantly between Cachaco (51.9 min) and the genotypes Mbwazirume (30.3 min) and Banksii (29.5 min; Figure 3A; Supplemental Figure S4 and Supplemental Table S2). This timing of A limitation was significantly correlated with the time to reach 95%, 90%, and 50% of steady-state g_s ($P < 0.001$, R^2 = 0.42–0.48), while there was no significant relation with the time to reach 95% or 90% of the maximum carboxylation rate of Rubisco ($V_{cmax,}$ Supplemental Figures S1 and S3). The timing to reach 95% of steady-state V_{cmax} was <20 min in all genotypes, while the timing to reach 95% of steady-state g_s was much longer and ranged between 41 and 69 min (Supplemental Figure S3 and Table S2). The durations of A limitation were also significantly correlated with the modeled time constant for g_s increase (K_i; $P < 0.001$, R^2 = 0.67; Supplemental Figure S1). The percentage limitation of A was significantly higher in Cachaco (20.6%) compared to the genotypes Mbwazirume (10.2%), Leite (10.2%), and Banksii (8.5%; Figure 3B) and was significantly related to both K_i and the time to reach 90% and 50% of steady-state g_s, confirming the impact of stomatal limitation on A (Supplemental Figure S1).

iWUE response to step-changes in light intensity

The step increase in light intensity induced an initial increase in A that was relatively larger than the increase in g_s.

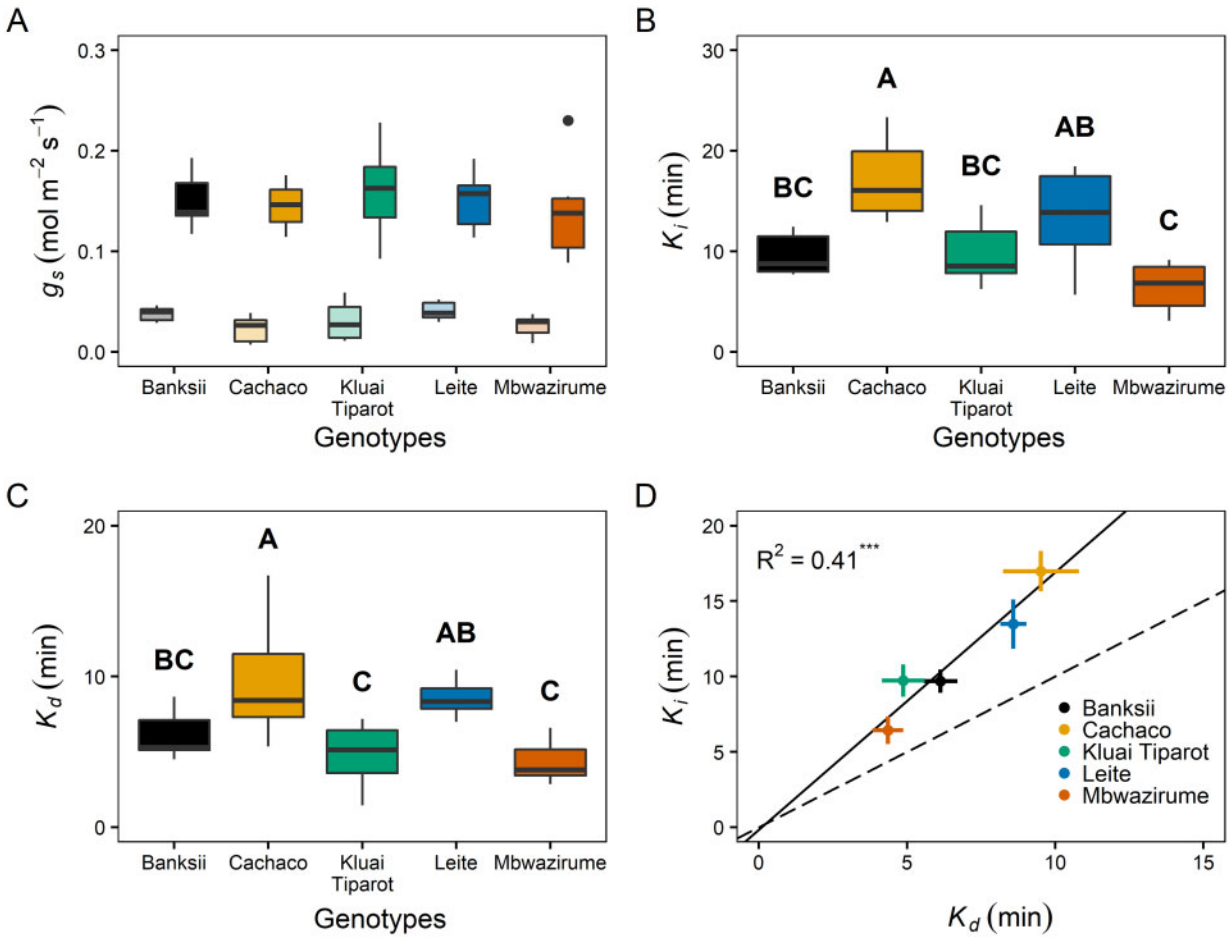

Figure 2 Modeled steady-state and light-induced variables of the g_s response to a step increase and decrease in light intensity between 100 and 1,000 µmol m^{-2} s^{-1} for five different banana genotypes (n = 7–8). A, Steady-state g_s at 100 ($g_{s,100}$ faded colors) and 1,000 µmol m^{-2} s^{-1} ($g_{s,1,000}$ bold colors). B, Time constant of g_s increase (K_i) for different genotypes. Different letters indicate significant differences between genotypes (post hoc Tukey HSD test, $P < 0.05$; A > B > C). C, Time constant of g_s conductance decrease (K_d) for different genotypes. Different letters indicate significant differences between genotypes (post hoc Tukey HSD test, $P < 0.05$; A > B > C). D, Significant correlation between K_i and K_d (Pearson's correlation, R^2 = 0.41, $P < 0.001$). K_i was significantly higher than K_d. The solid line shows the linear regression, the dashed line shows the 1:1 line. Points and error bars represent mean ± SE (n = 7–8). The bold middle line in boxplots represents the median. The box is confined by the first and third quartile and the whiskers extend to 1.5 times the interquartile distance. Points falling outside the whiskers are considered outliers and plotted as dots.

These responsiveness differences increased ¡WUE, reaching the maximum ¡WUE during the light period in all cases within 7.5 min (Supplemental Figure S5). After reaching a maximal value, ¡WUE decreased as both g_s and A gradually increased (Supplemental Figure S5). ¡WUE only stabilized when both A and g_s reached steady-state. The genotype Cachaco had a significantly higher mean ¡WUE during the high light period compared to Mbwazirume (Supplemental Figure S6). The mean ¡WUE during the high light period was significantly correlated with the time constant K_i and $SI_{max,i}$ with slower g_s responses resulting in higher ¡WUE (R^2 = 0.12 and 0.42, $P < 0.05$; Supplemental Figure S1). The reduction in light intensity from 1,000 to 100 µmol m^{-2} s^{-1} instantaneously lowered ¡WUE as A immediately declined because of light limitation (Supplemental Figure S5). The mean ¡WUE during this low light period was significantly higher in Kluai Tiparot, than in Leite (Supplemental Figure S6). The mean ¡WUE was significantly correlated to the stomatal closing variables K_d and $SI_{max,d}$ with faster g_s responses resulting in higher ¡WUE (R^2 = 0.36 and 0.26, $P < 0.001$; Supplemental Figure S1).

Stomatal anatomy

Banana has elliptical-shaped guard cells surrounded by four to six subsidiary cells (Rudall et al., 2017). Abaxial stomatal density, stomatal length, guard cell size, and subsidiary cell size were quantified from the leaf part enclosed in the gas exchange cuvette and significant differences between genotypes were observed (Supplemental Figure S7). Stomatal density and stomatal length were not correlated with any of the modeled light-induced g_s kinetics (Figure 4; Supplemental Figure S1). However, these correlations between anatomy and g_s kinetics were significant if the genotype Cachaco with the lowest g_s rapidity was not considered

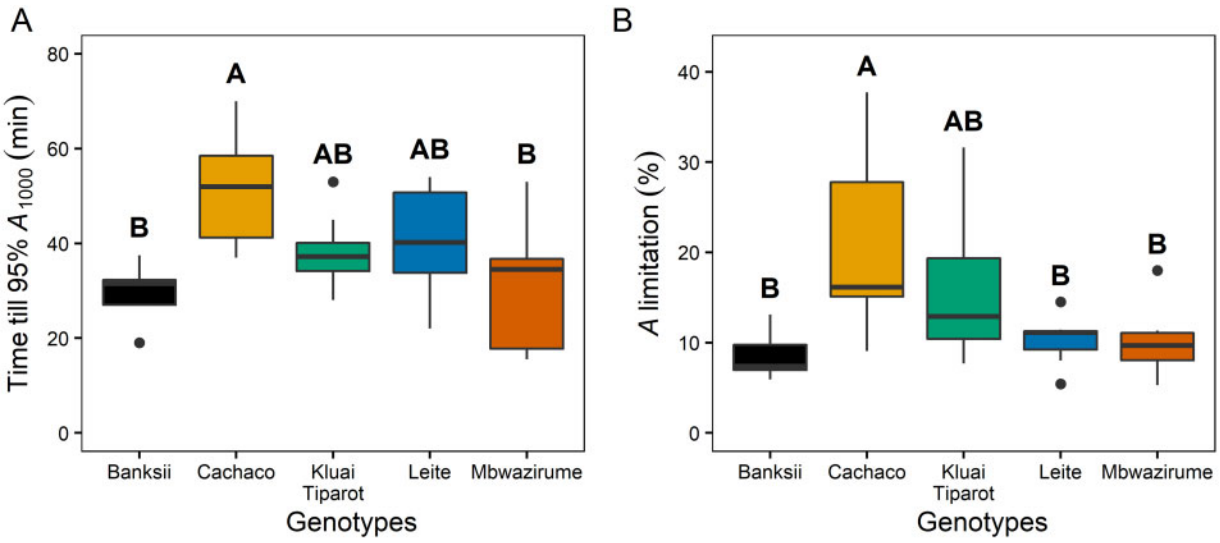

Figure 3 Limitation of *A* after the increase in light intensity from 100 to 1,000 µmol m^{-2} s^{-1}. A, Time to reach 95% of the steady-state *A* for five different banana genotypes. B, Percentage limitation of *A* after the increase in light intensity. Different letters indicate significant differences between genotypes (post hoc Tukey HSD test, $P < 0.05$; $n = 7–8$; A > B). The bold middle line in boxplots represents the median. The box is confined by the first and third quartile and the whiskers extend to 1.5 times the interquartile distance. Points falling outside the whiskers are considered outliers and plotted as dots.

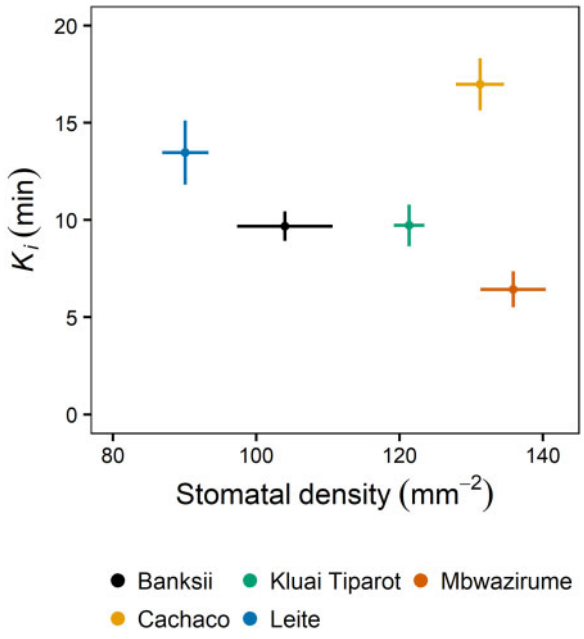

Figure 4 Relation between abaxial stomatal density and the time constant describing the speed of g_s increase after the light intensity increase from 100 to 1,000 µmol m^{-2} s^{-1}. There was no significant correlation (Pearson's correlation test), caused by the outlying genotype Cachaco. Points and error bars represent mean ± SE ($n = 7–8$).

(Figure 4). In this case, stomatal density was significantly correlated with the time constant *K* as well as the maximum slope of g_s response SI_{max} during both stomatal opening and closing ($P < 0.01$; $R^2 = 0.25–0.46$).

Whole-plant transpiration response at dawn

The significant differences in g_s speed at leaf level observed between the two extreme genotypes Cachaco and Mbwazirume were confirmed at the whole-plant level under a step increase in light intensity from darkness (Figure 5) and under a gradually increasing light intensity (Supplemental Figure S8). After the onset of light in the morning, the transpiration rate increased significantly faster in Mbwazirume compared to Cachaco (Figure 5, A and B; Supplemental Figure S8A). After a step increase in light intensity, a significant increase in transpiration rate was observed after *c.* 15 min in Mbwazirume, while in Cachaco this was only after 25 min (Figure 5, A and B). Similar faster increases in transpiration rate of Mbwazirume were observed under a gradually increasing light intensity (Supplemental Figure S8A). The temporal response of whole-plant transpiration rate to a step increase in light intensity was also modeled following the sigmoidal model (Eq. 1) and the time constants *Ki* differed significantly between genotypes (Supplemental Figure S9). Similar to the response at leaf level, Cachaco, had an average time constant K_i of 20 min, while Mbwazirume, had a K_i of 8.5 min (Supplemental Figure S9). The difference in transpiration responses was also reflected in the transpiration rate before and after dawn. The whole-plant transpiration rate did not differ significantly between both genotypes pre-dawn, but after the step change in light intensity, the transpiration rate was significantly higher in Mbwazirume for 90 min, whereafter both genotypes reached similar steady-state transpiration rates (Figure 5B). Likewise, the transpiration rate under gradually increasing light intensity did not differ pre-dawn, but was significantly higher in Mbwazirume after the onset of light (Supplemental Figure S8B).

Impact of diurnal light fluctuations on g_s, *A*, and ¡WUE

To evaluate the impact of g_s kinetics on diurnal *A* and ¡WUE, plants were subjected to fluctuating light intensities

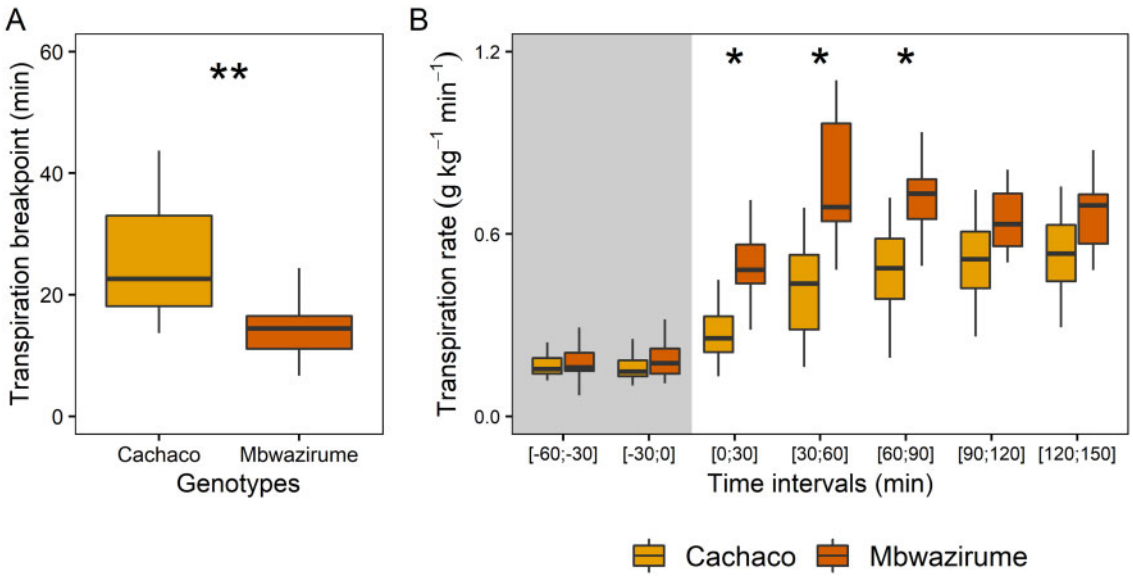

Figure 5 Gravimetric transpiration rate analysis of genotypes Cachaco and Mbwazirume at dawn after a step increase in light intensity from 0 to 120 µmol m^{-2} s^{-1}. A, A breakpoint was identified in whole-plant transpiration after the step increase in light intensity. The timing of the breakpoint in transpiration after dawn differed significantly between the genotype Cachaco and Mbwazirume (n = 24, $P < 0.01$, linear mixed-effects model with plant-specific and date-specific random effect). B, Transpiration rate after dawn increased faster in Mbwazirume compared to Cachaco. Before dawn transpiration rates did not differ significantly. Similarly transpiration rates do not differ significantly after 90 min (24 datapoints per time range for both Cachaco and Mbwazirume, * for $P < 0.05$, ** for $P < 0.01$, linear mixed-effects model with plant-specific and date-specific random effect). Gray areas indicate the time before dawn. The bold middle line in boxplots represents the median The box is confined by the first and third quartile and the whiskers extend to 1.5 times the interquartile distance.

and phenotyped over an entire diurnal period. Similar to the transpiration rate measured at the whole-plant level, the morning increase in g_s at leaf-level under gradually increasing light intensity was faster in Mbwazirume compared to Cachaco (Figure 6A). The time constant for the g_s increase (K_i) was significantly higher in Cachaco ($P < 0.005$; Figure 6B). However, the faster increase of g_s in Mbwazirume, did not result in increased A (Figure 6C). Maximum potential A values at specific light intensities were determined from light response curves and compared to those measured under the diurnal conditions. Under the gradual increasing light intensities experienced in the morning, maximum A values were achieved, indicating there was no g_s limitation under these light-limiting conditions (Figure 7). A similar A with lower g_s during the morning, led to a significantly higher mean $_i$WUE in Cachaco ($P < 0.05$, Figure 6D).

Throughout the day, g_s kinetics were in most cases significantly faster for the genotype Mbwazirume compared to Cachaco (Figure 8A), again confirming the previously observed kinetics (Figures 2 and 5). However, under fluctuating light conditions g_s kinetics were dependent on the magnitude of light intensity change, g_s values prior to the light intensity change, and the time of the day (Figure 8A). During the afternoon, there was a setback in kinetics: the absolute g_s and the g_s responses to light were damped (Figures 7 and 8). Simultaneously, A decreased greatly in the afternoon, which could be mainly attributed to a reduction in g_s. The limitation of A in the afternoon was 3 times higher in Cachaco (52.6%) compared to Mbwazirume (17.5%; Figures 7 and 9D). The reduction of g_s in the afternoon resulted in a significantly lower average diurnal g_s (Figure 9A) which translated into a greater diurnal $_i$WUE in Cachaco compared to Mbwazirume (Figures 8C and 9C).

Discussion

Stomatal behavior greatly limits *A* in banana

Step changes in light intensity have been shown to induce an uncoupling of A and g_s in many species (Barradas and Jones, 1996; Lawson and Blatt, 2014; McAusland et al., 2016; Faralli et al., 2019a). However, all banana genotypes maintain a tight coupling between A and g_s following a step increase in light intensity (Figure 1). This indicates a strong stomatal control of A, which is demonstrated by diffusional limitations accounting for >89% of A limitation (Supplemental Figure S3A). This high stomatal limitation of A is explained by the slow g_s response (Figures 1 and 2) relative to the faster biochemical activation. The time required for biochemical activation was much lower and not correlated with the time for steady-state A and g_s (Supplemental Figure S3). Similar to Deans et al. (2019a) and De Souza et al. (2020), the speed of changes in g_s was the predominant limitation of A. This behavior shows that banana strongly controls stomatal aperture, resulting in water conservation at the expense of potential carbon gain, which supports the early work of Aubert and Catsky (1970). This prioritizing of water conservation in banana can be

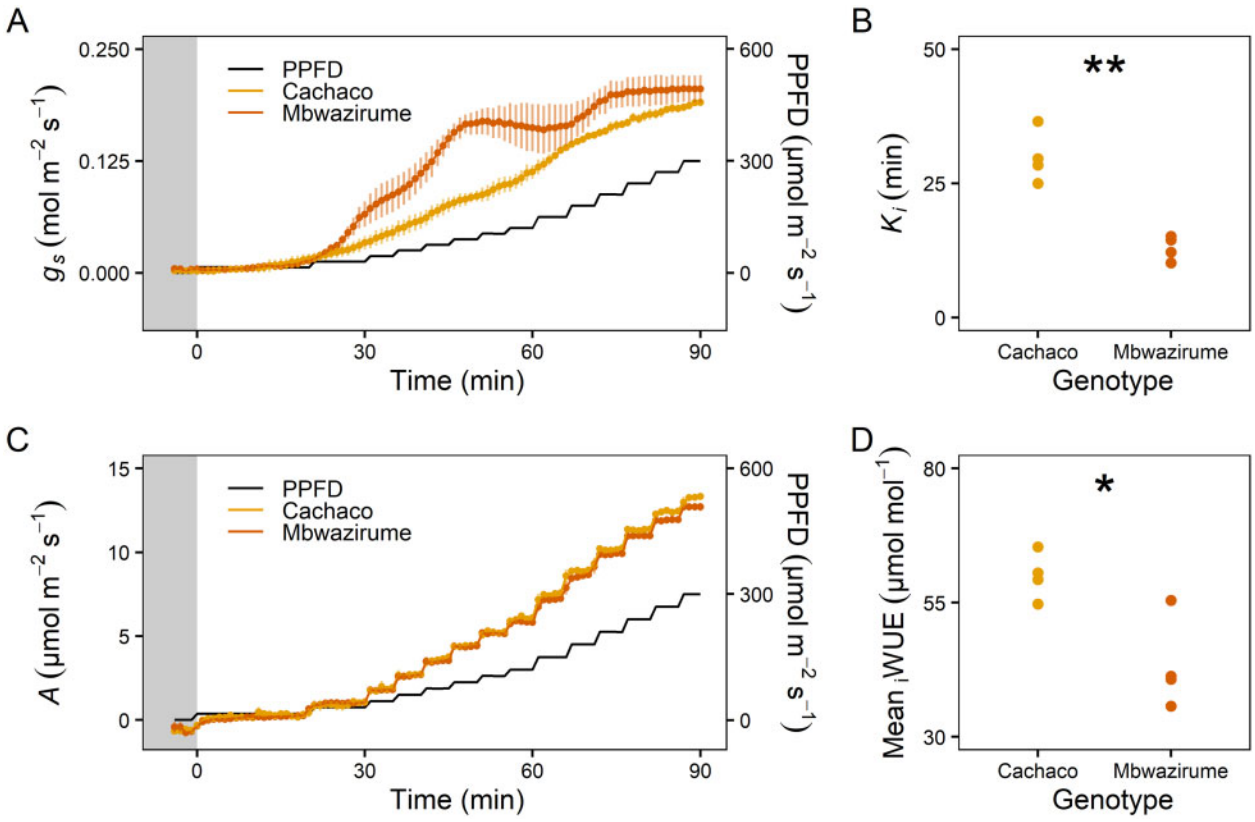

Figure 6 Morning response of g_s and A of the genotypes Cachaco and Mbwazirume. A, Time course of the g_s response to a gradual increase in light intensity at dawn (black line). Data are the mean ± SE (n = 4). B, The time constant of g_s increase (K_i) during the first 90 min after dawn was significantly higher in Cachaco. C, The difference in g_s rapidity at dawn did not result in different A between both genotypes. Data represent the mean ± SE (n = 4). D, The mean $_i$WUE during the first 90 min after dawn was significantly higher in Cachaco compared to Mbwazirume. The gray area indicates the time before dawn. (Student's t test, *$P < 0.05$, ** $P < 0.01$).

explained by its intrinsic need to maintain a high leaf water potential (Turner and Thomas, 1998).

Diversity in light-induced stomatal responses

Stomatal responses to changes in light intensity have been shown to vary at an inter- and intra-specific level (Vico et al., 2011; Drake et al., 2012; McAusland et al., 2016; Qu et al., 2016; De Souza et al., 2020; Durand et al., 2020). A higher steady-state g_s has been linked with faster light-induced g_s responses (Drake et al., 2012; Kaiser et al., 2016; McAusland et al., 2016; Wachendorf and Küppers, 2017; Sakoda et al., 2020). Although the differences observed in steady-state g_s values between banana genotypes were not significant, their g_s kinetics differed strongly (Figure 2). These results suggest that other factors such as stomatal anatomy, hydraulic conductance and membrane transporters are involved in determining the rapidity of changes in g_s.

The banana B genome is often related to drought tolerance because of its center of origin and its natural occurrence in drier habitats under full sunlight (Perrier et al., 2011; Janssens et al., 2016; Eyland et al., 2021). Within the investigated banana genotypes, we observed significant differences in the speed of increase and decrease in g_s (Figure 2, B and C). However, differences across genotypes were not explained by their genomic constitution (see "Materials and Methods" section), which is in agreement with the wide diversity of transpiration phenotypes observed irrespective of genomic constitution (van Wesemael et al., 2019).

Consistent with previous works in other species (Vico et al., 2011; McAusland et al., 2016; Faralli et al., 2019a), the speed of g_s increase and decrease was significantly correlated (Figure 2D). Decreases in g_s were faster than opening in all banana genotypes (Figure 2D), which is not the case for all crops (McAusland et al., 2016; Qu et al., 2016). The faster g_s closure again indicates that banana prioritizes water conservation over maximization of carbon uptake.

The two most extreme genotypes Cachaco and Mbwazirume, with the slowest and fastest g_s responses, respectively, also showed at the whole-plant level differences in the light-induced speed of transpiration rate increase (Figure 5; Supplemental Figures S8 and S9). This finding suggests that despite possible differences in g_s control of water loss at different locations of the leaf (Matthews et al., 2017) and across leaves of different ages (Urban et al., 2008) genotype-specific responses are still maintained. Leaf-level measurements of light-induced g_s kinetics are thus in line with whole-plant responses. To our knowledge, this is the first report confirming stomatal kinetics at the whole-plant

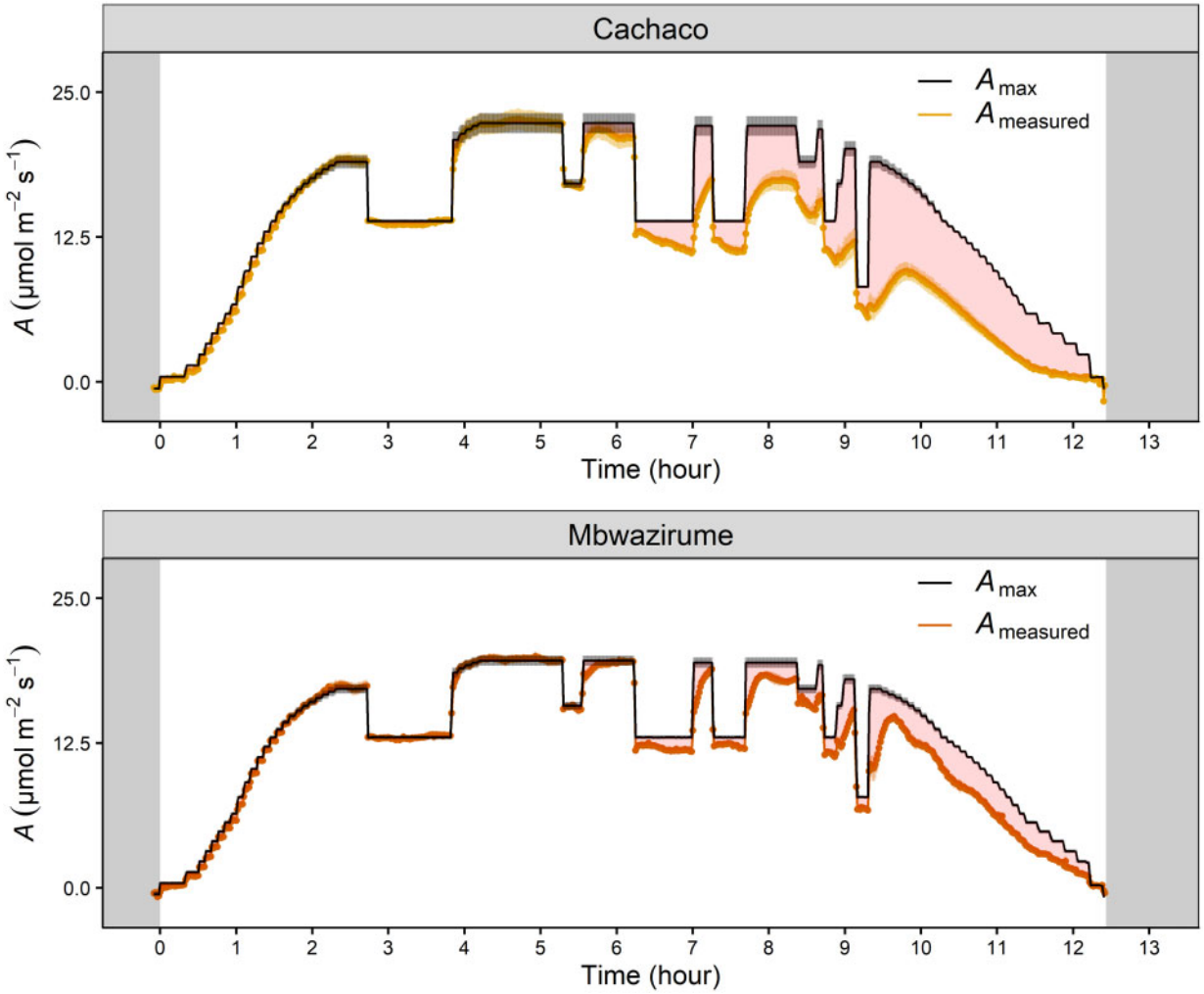

Figure 7 Mean diurnal time course of measured A ($A_{measured}$ and maximal A (A_{max}, black line) under fluctuating light conditions for Mbwazirume and Cachaco. The A_{max} at each light intensity was determined by a modeled light response curve. The nonrectangular hyperbola-based model of Prioul and Chartier (1997) was optimized as described by Lobo et al. (2013). Grey areas indicate times of darkness, red areas indicate the difference between maximal A and measured A. Data are the mean ± SE (n = 4).

level. The genotype-specific difference in whole-plant transpiration responses at dawn was validated at the leaf level with g_s increasing faster in Mbwazirume under gradually increasing light intensity (Figure 6A). This faster g_s increase in Mbwazirume did not result in higher A, indicating that at dawn, under gradually increasing low light intensities, g_s was not limiting A and was higher than necessary for maximal A (Figures 6 and 7). These results demonstrate that the impact of g_s kinetics on A and $_i$WUE depends on the time of the day and the light conditions. The uncoupling of g_s and A under increasing light conditions at dawn was not beneficial for carbon uptake. Gosa et al. (2019) called this period after dawn in tomato the golden hour because in dry climates it is the time of the day with the highest g_s. Later in the day, VPDs become too high, restricting g_s (Gosa et al., 2019). Breeding for an even higher g_s during this golden hour was suggested to improve plant productivity. However, care must be taken to breed for an improved morning CO_2 uptake, rather than for a high g_s with associated uncoupling of A and g_s. Although the absolute water loss resulting from excessive morning g_s might be relatively low because of low evaporative demands at dawn (Chaves et al., 2016), it may lead to a crucial decrease in overall plant water status.

Despite the confirmed genotypic differences in stomatal kinetics, the impact of g_s kinetics on A and $_i$WUE before noon hardly differed between the genotypes Cachaco and Mbwazirume under field-mimicking light conditions (Figures 7 and 8). This could be explained by lower amplitudes of light switches compared to a single step change in light intensity and/or g_s values not being at steady-state prior to changing light intensity. The genotype-specific speed of the g_s response observed under a single step change in light intensity did not explain the diurnal $_i$WUE, indicating that g_s kinetics only partially affect diurnal WUE and carbon gain (Figure 9, B and C). The absolute g_s and the g_s responses to light decreased strongly in the afternoon, and this effect was more pronounced in the genotype Cachaco (Figures 7 and 8A). The 3 times higher

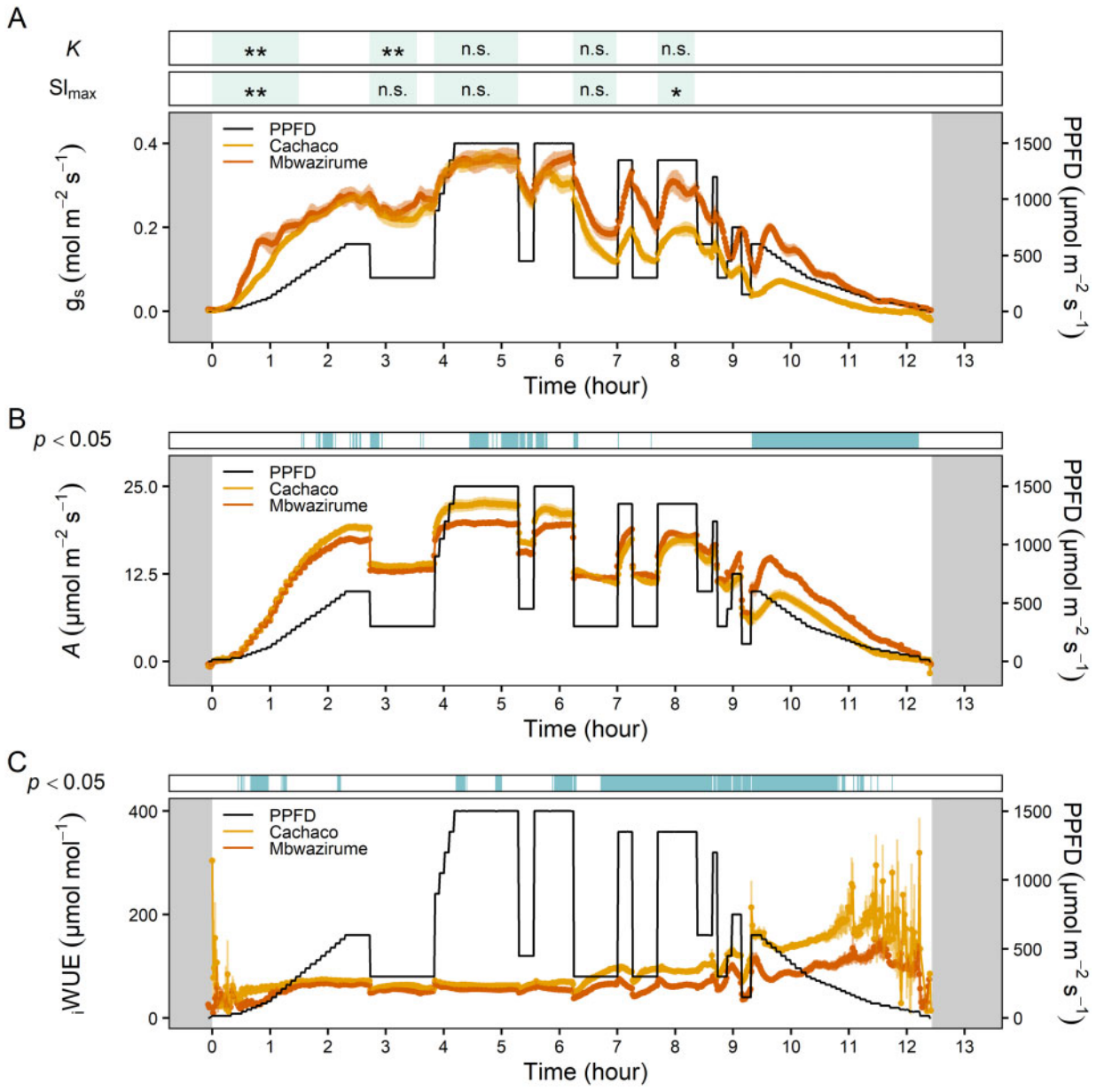

Figure 8 Diurnal time course of gas exchange parameters of the genotypes Mbwazirume and Cachaco under fluctuating light conditions. A, g_s, (B) A, and (C) $_i$WUE. The light intensity fluctuated throughout the day (black line). The significance of the time constant of g_s increase or decrease (K) and the maximal slope of g_s increase or decrease (SI_{max}) is shown (Student's t test, $^*P < 0.05$ and $^{**}P < 0.01$ for faster g_s rapidity in Mbwazirume compared to Cachaco). Throughout the day, g_s kinetics were faster for the genotype Mbwazirume compared to Cachaco, but differences were dependent on the target light intensity, the magnitude of change, the g_s prior to the intensity change, and the time of the day. Gray areas indicate times of darkness. Green areas indicate the analyzed time frame of the g_s rapidity response. Blue areas indicate time points with significant differences in A or $_i$WUE between both genotypes (Student's t test, $P < 0.05$). Data are the mean ± SE ($n = 4$).

afternoon limitation of A in the genotype Cachaco compared to Mbwazirume, resulted in a significantly higher diurnal $_i$WUE (Figure 9, C and D). The genotype Cachaco with the slowest g_s kinetics thus achieved the highest $_i$WUE, showing that not only g_s speed but also the g_s diurnal pattern determines the overall WUE and carbon gain. Although the mechanism behind the afternoon g_s reduction remains largely unknown, it is commonly hypothesized to be related to circadian regulation of ABA sensitivity and associated endogenous signals regulating the clock, such as feedback loops from photosynthate accumulation (Mencuccini et al., 2000; Haydon et al., 2013; Delorge et al., 2014; Resco de Dios and Gessler, 2018). We show that under fluctuating light conditions this intrinsic diurnal pattern of absolute g_s decrease and g_s light responsivity reduction is decisive for diurnal $_i$WUE (Figure 9C).

Impact of stomatal anatomy on responses

Stomatal density, as well as the size, have been reported to affect g_s kinetics (Hetherington and Woodward, 2003; Drake

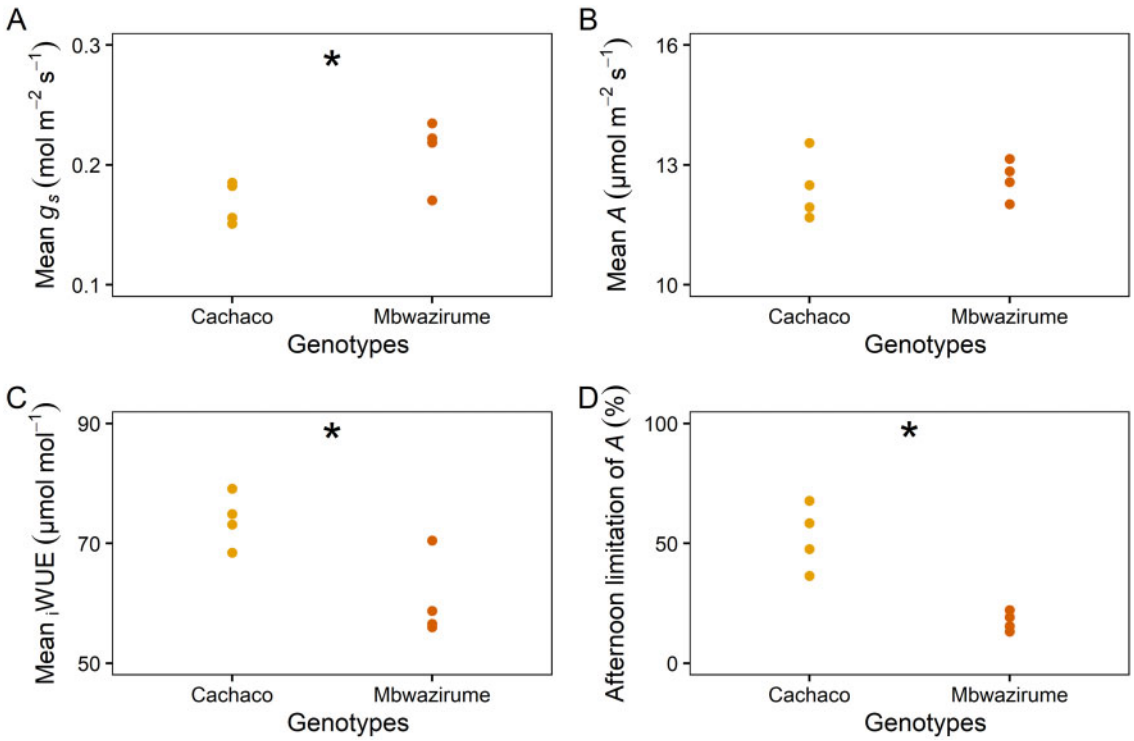

Figure 9 Average diurnal gas exchange parameters of the genotypes Mbwazirume and Cachaco under fluctuating light conditions illustrated in Figure 8. A, g_s, (B) A, and (C) iWUE. D, The percentage limitation of A during the afternoon (>6 h after light onset). (Student's t test, * $P < 0.05$, $n = 4$).

et al., 2012; Raven, 2014; Sakoda et al., 2020). However, McAusland et al. (2016) and Faralli et al. (2019a) reported no or only a weak inter- and intra-specific correlation between stomatal anatomy and light-induced g_s kinetics. We confirmed that stomatal density and size were not correlated with the g_s kinetics (Figure 4; Supplemental Figure S1). Remarkably, the genotype with the slowest increase in g_s, Cachaco had the second highest density and the smallest stomata. Without this genotype a significant correlation between density and the speed of g_s increase and decrease was observed (Figure 4). This exception suggests that the surface-to-volumes ratios are not always directly related to stomatal speed as this assumes uniform ion transport activity per surface area (Lawson and Blatt, 2014).

Conclusion

Our findings show that there is diversity in g_s rapidity to light within closely related banana genotypes and that slow stomatal responses and not biochemical activation greatly limit A. The priority of banana for water saving is shown by strong stomatal control of A and faster decrease in g_s than increase. The observed diversity in g_s rapidity was not related to stomatal anatomy and therefore suggests that variation is rather driven by functional components. We show here for the first time that the g_s rapidity observed at the leaf level can also be found at the whole-plant level. However, under fluctuating light conditions, g_s rapidity is only one of the many physiological factors determining overall plant WUE and carbon gain.

Materials and methods

Experiment 1: Leaf gas exchange response to a step-change in light intensity

Plant material and growth conditions

Banana plants (*Musa* spp.) were obtained through the International Musa Transit Center (ITC, Bioversity International), hosted at KU Leuven, Belgium. Plants of five genotypes from different subgroups were selected: Banksii (subgroup Banksii, AA genome, ITC0623), Cachaco (Bluggoe, ABB genome, ITC0643), Kluai Tiparot (Kluai Tiparot, ABB genome, ITC0652), Leite (Rio, AAA genome, ITC0277), and Mbwazirume (Mutika-Lujugira, AAA genome, ITC1356). Plants were grown in 800 mL containers filled with peat-based compost (Levingtons F2S, UK) under 350 µmol m^{-2} s^{-1} photosynthetic photon flux density (PPFD) in a 12-h: 12-h light: dark cycle with temperature and relative humidity at 26 ± 1°C and 70 ± 10%, respectively. Plants were well-watered and starting from Week 3 a Hoagland nutrient solution was added. Measurements were performed when plants were fully acclimated and 7 weeks old.

Leaf gas exchange measurements

A and g_s to water were measured every 30 s on the middle of the second youngest fully developed leaf using an LI-6400XT infrared gas analysis and dew-point generator model

LI-610 (LI-COR, Lincoln, NE, USA). Light was applied by an integrated LED light source. The leaf cuvette maintained a CO_2 concentration of 400 µmol mol^{-1}, a leaf temperature of 25°C, and a VPD of 1 kPa. All measurements were performed before 14:00 h to avoid circadian influences.

Stomatal response to a step change in light intensity

The light intensity was kept at 100 µmol m^{-2} s^{-1} until A and g_s were stable for 10 min. Once steady-state was reached, light intensity was increased to 1,000 µmol m^{-2} s^{-1} for 90 min. Then, light intensity was lowered back to 100 µmol m^{-2} s^{-1} for 30 min.

The increase in g_s after the increase in light intensity and the decrease in g_s after the decrease in light intensity followed a sigmoidal pattern and was modeled using the nonlinear sigmoidal model described in Vialet-Chabrand et al. (2017):

$$g_s = (g_{s,1000} - g_{s,100})\, e^{-e^{\left(\frac{\lambda - t}{K} + 1\right)}} + g_{s,1000} \quad \text{(Eq. 1)}$$

With g_s the g_s at time t, K the time constant for rapidity of g_s response (min), λ the lag time of the sigmoidal curve (min), $g_{s,100}$ and $g_{s,1,000}$ (mol m^{-2} s^{-1}) the steady-state g_s at 100 and 1,000 µmol m^{-2} s^{-1}, respectively. Parameter values were estimated for each individual plant using nonlinear model optimization in R version 3.4.3. K_i indicates the g_s increase time constant, K_d the g_s decrease time constant. The maximum slope of g_s during opening and closing was calculated and defined as Sl_{max}. $_i$WUE was calculated as $_i$WUE = A/g_s. Outlying values (0.5% quantile; $_i$WUE < 0 or > 400 µmol mol^{-1}) caused by low g_s were discarded for plotting.

Stomatal and biochemical limitation analysis

A was considered to be limited until 95% of steady-state A at 1,000 µmol m^{-2} s^{-1} was reached (McAusland et al., 2016). The percentage of limitation of A was calculated by comparing the measured A with the maximal steady-state A under 1,000 µmol m^{-2} s^{-1} according to McAusland et al. (2016):

$$\text{Limitation of } A\ (\%) = \frac{\int_0^t \sum (A_{max} - A_{measured})}{\int_0^{90} \sum A_{measured}} \quad \text{(Eq. 2)}$$

With A_{max} the value reached at 95% of steady-state A under 1,000 µmol m^{-2} s^{-1}, $A_{measured}$ the measured A and t the time where 95% of steady-state A is reached.

The delay in obtaining maximum potential A under 1,000 µmol m^{-2} s^{-1} is determined by the stomatal opening speed as well as the rate of biochemical activation. The activation rate of Rubisco is the main biochemical limiting component during step changes in light exceeding several minutes (Mott and Woodrow, 2000; Way and Pearcy, 2012). To quantify the relative contributions of biochemical and stomatal limitations a differential method was applied (Jones, 1985; Wilson et al., 2000; Grassi and Magnani, 2005; Deans et al., 2019b). As explained by Deans et al. (2019b), the forgone A because of biochemical and stomatal limitation was calculated as:

$$dA_{biochem} = \frac{\partial A}{\partial V_{cmax}} dV_{cmax} \quad \text{(Eq. 3)}$$

and

$$dA_{stom} = \frac{\partial A}{\partial g_{sc}} dg_{sc} \quad \text{(Eq. 4)}$$

where V_{cmax} is the maximum velocity of Rubisco for carboxylation and g_{sc} the g_s to CO_2. V_{cmax} at every time point was calculated by solving the Rubisco-limited A as described by Farquhar et al. (1980) for V_{cmax}:

$$V_{cmax} = \frac{(A + R_d)(C_i + K_m)}{(C_i - \Gamma^*)} \quad \text{(Eq. 5)}$$

where C_i is the CO_2 concentration in the intercellular airspaces of the leaf. R_d represents the mitochondrial respiration for which average dark respiration rates were used. Γ^* is the photorespiratory compensation point and K_m is the effective the Rubisco Michaelis–Menten constant for CO_2 under 21% O_2. Values for Γ^* and K_m were taken as the average for C3 species at 25°C as described by Hermida-Carrera et al. (2016), 41.2 and 529.4 µmol mol^{-1}, respectively. Mesophyll conductance to CO_2 was assumed to be infinite. g_{sc} at every time point was calculated as:

$$g_{sc} = \frac{g_s}{1.6} \quad \text{(Eq. 6)}$$

The relative stomatal limitation (σ_{stom}) was then calculated as:

$$\sigma_{stom} = \frac{\int_0^t dA_{stom}\, dt}{\int_0^t dA_{biochem}\, dt \int_0^t dA_{stom}\, dt} \quad \text{(Eq. 7)}$$

where t represents the time where 95% of steady-state A under 1,000 µmol m^{-2} s^{-1} was reached. Timings representing the g_s and A increase were calculated at 95%, 90%, and 50% of steady-state values under 1,000 µmol m^{-2} s^{-1}. Timings for V_{cmax} were calculated at 95% and 90% of steady-state values.

Stomatal anatomy measurements

Stomatal impressions of the abaxial surface of the leaf were made when stomata were completely closed using impression material. Impression was made by applying dental polymer according to the protocol of Weyers and Johansen (1985), followed by covering the polymer with nail varnish and placement on a microscope slide. Impressions were only taken from the abaxial side, because stomatal densities are generally 75% higher compared to the adaxial side in banana, therefore majorly determining gas exchange as shown

by Brun (1961). Stomatal anatomy was quantified using an EVOS digital inverted microscope. Stomatal density was determined in three microscopic fields of views of 1.12 mm^2 captured with a 10× objective lens (54–117 stomata per field of view). Guard cell length (μm), guard cell size (mm^2), and lateral subsidiary cell size (mm^2) were determined in three microscopic field of views of 0.07 mm^2 captured with a 40× magnification, respectively (four to seven stomata per field of view). Measurements were performed in ImageJ software (http://rsb.info.nih.gov/ij).

Experiment 2: Whole-plant transpiration response at dawn

Plant material and growth conditions greenhouse experiment

For the genotypes Cachaco and Mbwazirume, 12 plants were grown for 7 weeks in a greenhouse prior to the experiment. Plants were grown in 10 L containers filled with peat-based compost. At the start of the experiments, the six most homogenous plants per genotype were selected based on leaf area. Weight of each plant was followed by a multi-lysimeter setup of high precision balances, registering the weight every 60 s (1 g accuracy, Phenospex, Heerlen, Netherlands). The soil was covered by plastic to avoid evaporation and ensure only waterloss through transpiration. The transpiration rate was calculated by differentiating the raw weight data over time. The soil water content was determined by subtracting the plastic pot weight, the dry soil weight, and the plant weight from the total weight measurement. Dry soil weight was calculated as a function of the soil volume (bulk density = 0.2267 g cm^{-3}). Leaf area was calculated by weekly top view imaging and model over time by a power-law function (Paine et al., 2012):

$$leaf\ area = k + a * \text{days}^b \quad \text{(Eq. 8)}$$

The daily plant weight was estimated from the projected leaf area using genotype-specific correlations ($n > 50$; $R^2 \geqslant 0.94$). Plants were watered with a nutrient solution during the night and kept at well-watered conditions. Radiation was collected every 5 min via a sensor (Skye instruments, Llandrindod Wells, UK) inside the greenhouse. Supplemental lighting of 14 W m^{-2} at plant level was provided when solar radiation was <250 W m^{-2} during the daytime. Temperature and relative humidity data were collected using six data loggers (Trotec, Heinsberg, Germany) registering data every 5 min. The onset of light was defined as the moment when intensity increased >2 W m^{-2}.

Plant material and growth conditions controlled environment experiment

For the genotypes Cachaco and Mbwazirume, three plants were grown in a growth chamber with relative humidity of 70% and temperature of 24°C. Plants were grown hydroponically in containers with 350 mL medium (see van Wesemael et al. (2019) for specific nutrient composition) and placed under adjustable LED panels (LuminiGrow 600R1; Lumini technology Co. Ltd., Zhejiang, China) providing 120 μmol m^{-2} s^{-1} in a 12/12-h light/dark cycle. Plants were 5 weeks old at the start of the experiment and weighted prior to the experiment to normalize for plant mass. Biomass was again measured after 8 d, at the end of the experiment. Water loss of each plant was followed by a multi-lysimeter setup of high precision balances (0.01 g accuracy; Kern, Balingen, Germany). Balances were connected to a computer registering the weight every 10 s.

Experiment 3: Impact of diurnal light fluctuations on g_s, A, and $_i$WUE

Plant material and growth conditions

Four plants of the genotypes Cachaco and Mbwazirume were grown in a greenhouse. Plants were grown in 4 L containers filled with peat-based compost and maintained under well-watered conditions. After 8 weeks plants were moved to a growth chamber with relative humidity 70 ± 15% and temperature 28 ± 2°C.

Leaf gas exchange measurements

A and g_s were measured every minute on the middle of the second youngest fully developed leaf using an LI-6800 infrared gas analyzer (LI-COR, Lincoln, NE, USA). The leaf cuvette maintained a CO_2 concentration of 400 μmol mol^{-1}, a leaf temperature of 28°C and a VPD of 1 kPa. The light intensity was programmed to fluctuate throughout the day. Plants were placed under adjustable LED panels (LuminiGrow 600R1; Lumini technology Co. Ltd.,Zhejiang, China) that mimicked light fluctuations inside the LI-6800 leaf cuvette. The g_s response was described using the nonlinear sigmoidal model of Vialet-Chabrand et al. (2013) where light or dark steps were sufficiently long for model optimization (Eq. 1). A light response curve with A in function of PPFD was modeled for each individual based on A values recorded during the first 6 h of the day that was not limited by g_s. The non-rectangular hyperbola-based model of Prioul and Chartier (1977) was optimized as described C Lobo et al. (2013):

$$A = \frac{PPFD * \Phi_0 + A_{max} - \sqrt{\Phi_0 * PPFD + A_{max}2 - 4\theta * \Phi_0 * PPFD * A_{max}}}{2\theta} - R_n \quad \text{(Eq. 9)}$$

With A the photosynthetic rate (μmol m^{-2} s^{-1}), PPFD (μmol m^{-2} s^{-1}), Φ_0 the quantum yield at PPFD of 0 μmol m^{-2} s^{-1} (μmol μmol^{-1}), A_{max} the absolute maximum photosynthetic rate (μmol m^{-2} s^{-1}), θ the dimensionless convexity factor and R_n the dark respiration (μmol m^{-2} s^{-1}).

The percentage of limitation of A by g_s during the afternoon (>6 h after light onset) was calculated by estimating the maximal potential A without g_s limitation and comparing it with the measured A (Eq. 2).

Statistical analysis and data processing

All data processing and statistical analysis were carried out in R version 3.4.3. Genotypic differences were tested by applying one-way analysis of variance with a post hoc Tukey HSD test. Segmented regression was performed on the whole-plant transpiration between −90 and 90 min relative to the onset of light. Data with no significant segmented regression (*P*-value Davies Test <0.05, segmented R package, 7.5% of the data) and negative slopes (2.5% of the data) were removed. Transpiration rate was calculated as the mean water loss every 30 min. To use the sigmoidal model (1) on whole-plant transpiration data, 1 min weight measurements were smoothed according to the Savitzky and Golay (1964) method with a filtering window of 21 and a fourth-order polynomial. Each day of whole-plant transpiration responses was regarded as a new replicate by incorporating a plant-specific factor and a date-specific factor as a random effect in a linear mixed model.

Supplemental data

The following materials are available in the online version of this article.

Supplemental Figure S1. Correlation matrix of gas exchange and stomatal anatomy variables.

Supplemental Figure S2. Maximum slope of g_s response (Sl_{max}) to an increase in light intensity from 100 μmol m^{-2} s^{-1} to 1,000 μmol m^{-2} s^{-1} and to a decrease in light intensity from 1,000 μmol μmol m^{-2} s^{-1} to 100 μmol m^{-2} s^{-1}

Supplemental Figure S3. Stomatal limitation of *A* and timings until steady-state values of *gs*, *A*, and maximum velocity of Rubisco for carboxylation (V_{cmax}) were reached after an increase in light intensity from 100 μmol m^{-2} s^{-1} to 1,000 μmol m^{-2} s^{-1}.

Supplemental Figure S4. Increase in *A* after increasing the light intensity from 100 μmol m^{-2} s^{-1} to 1,000 μmol m^{-2} s^{-1}. A was considered limited until 95% of steady-state *A* was reached.

Supplemental Figure S5. Response of iWUE and the intracellular CO2 to a step increase and decrease in light intensity from 100 to 1,000 μmol m^{-2} s^{-1} and back.

Supplemental Figure S6. Mean iWUE after the increase in light intensity from 100 to 1,000 μmol m^{-2} s^{-1} and the decrease to 100 μmol m^{-2} s^{-1} afterward.

Supplemental Figure S7. Stomatal density, stomatal length, guard cell size, subsidiary cell size, and proportion of subsidiary cells of the five banana genotypes.

Supplemental Figure S8. Gravimetric transpiration rate analysis of genotypes Cachaco and Mbwazirume under gradual increasing light intensity.

Supplemental Figure S9. Modeled time constant (Ki) for the whole-plant transpiration rate increase of genotypes Cachaco and Mbwazirume after a step increase in light intensity from 0 to 120 μmol m^{-2} s^{-1}.

Supplemental Table S1. Modeled steady-state and light-induced variables of the *gs* response to a step increase and decrease in light intensity from 100 to 1,000 μmol m^{-2} s^{-1} for five different banana genotypes.

Supplemental Table S2. Time to reach 95%, 90%, and 50% of steady-state *A*, *gs*, and V_{cmax} after a step increase in light intensity from 100 to 1,000 μmol m^{-2} s^{-1} for five different banana genotypes.

Acknowledgment

The authors would like to thank Edwige André for the plant propagation and growth; Hendrik Siongers, Stan Blomme, Loïck Derette, Simon Costers, and Kaat Hebbelinck for technical assistance during plant growth and phenotyping; Silvere Vialet-Chabrand and Phil Davey for their technical assistance during the step changes in light intensity experiment.

Funding

This work was funded by the Global Crop Diversity Trust project "Crop wild Relatives Evaluation of drought tolerance in wild bananas from Papua New Guinea" (grant no: GS15024), by the CGIAR Research Program Roots, Tubers and Bananas, by the COST Action Phenomenall FA 1306 and by the Belgian Development Cooperation project "More fruit for food security: developing climate-smart bananas for the African Great Lakes region." TL would like to acknowledge BBSRC for support (grant nos: BB/T004274/1; BB/S005080/1).

Conflict of interest statement. The authors declare that the research was conducted in the absence of any commercial or financial relationships that could be construed as a potential conflict of interest.

References

Acevedo-Siaca LG, Coe R, Wang Y, Kromdijk J, Quick WP, Long SP (2020) Variation in photosynthetic induction between rice accessions and its potential for improving productivity. New Phytol **227**: 1097–1108

Assmann SM, Shimazaki KI (1999) The multisensory guard cell. Stomatal responses to blue light and abscisic acid. Plant Physiol **119**: 809–815

Aubert B, Catsky J (1970) The onset of photosynthetic CO2 influx in banana leaf segments as related to stomatal diffusion resistance at different air humidities. Photosynthetica **4**: 254–256

Barradas VL, Jones HG (1996) Responses of CO2 assimilation to changes in irradiance: laboratory and field data and a model for beans (Phaseolus vulgaris L.). J Exp Bot **47**: 639–645

Brun W (1961) Photosynthesis & transpiration from upper & lower surfaces of intact banana leaves. Plant Physiol **36**: 399–405

Chaves MM, Costa JM, Zarrouk O, Pinheiro C, Lopes CM, Pereira JS (2016) Controlling stomatal aperture in semi-arid regions—The dilemma of saving water or being cool? Plant Sci **251**: 54–64

Deans RM, Brodribb TJ, Busch FA, Farquhar GD (2019a) Plant water-use strategy mediates stomatal effects on the light induction of photosynthesis. New Phytol **222**: 382–395

Deans RM, Farquhar GD, Busch FA (2019b) Estimating stomatal and biochemical limitations during photosynthetic induction. Plant Cell Environ **42**: 3227–3240

Delorge I, Janiak M, Carpentier S, Van Dijck P (2014) Fine tuning of trehalose biosynthesis and hydrolysis as novel tools for the generation of abiotic stress tolerant plants. Front Plant Sci. **5**: 147

Drake PL, Froend RH, Franks PJ (2012) Smaller, faster stomata: scaling of stomatal size, rate of response, and stomatal conductance. J Exp Bot **64**: 495–505

Durand M, Brendel O, Buré C, Le Thiec D (2020) Changes in irradiance and vapour pressure deficit under drought induce distinct stomatal dynamics between glasshouse and field-grown poplars. New Phytol **227**: 392–406

Eyland D, Breton C, Sardos J, Kallow S, Panis B, Swennen R, Paofa J, Tardieu F, Welcker C, Janssens SB, et al. (2021) Filling the gaps in gene banks: collecting, characterizing, and phenotyping wild banana relatives of Papua New Guinea. Crop Sci **61**: 137–149

Faralli M, Cockram J, Ober E, Wall S, Galle A, Rie J, Van, Raines C, Lawson T, Casson SA, Christian C, et al. (2019a) Genotypic, developmental and environmental effects on the rapidity of gs in wheat: impacts on carbon gain and water-use efficiency. Front Plant Sci **10**: 1–13

Faralli M, Matthews J, Lawson T (2019b) Exploiting natural variation and genetic manipulation of stomatal conductance for crop improvement. Curr Opin Plant Biol **49**: 1–7

Farquhar GD, Caemmerer S, Berry JA (1980) A biochemical model of photosynthetic CO_2 assimilation in leaves of C_3 species. Planta **149**: 78–90

Farquhar GD, Sharkey TD (1982) Stomatal conductance and photosynthesis. Annu Rev Plant Physiol **33**: 317–345

Fischer RA, Rees D, Sayre KD, Lu ZM, Condon AG, Larque Saavedra A (1998) Wheat yield progress associated with higher stomatal conductance and photosynthetic rate, and cooler canopies. Crop Sci **38**: 1467–1475

Franks PJ (2006) Higher rates of leaf gas exchange are associated with higher leaf hydrodynamic pressure gradients. Plant, Cell Environ **29**: 584–592

Franks PJ, Farquhar GD (2007) The mechanical diversity of stomata and its significance in gas-exchange control. Plant Physiol **143**: 78–87

Gosa SC, Lupo Y, Moshelion M (2019) Quantitative and comparative analysis of whole-plant performance for functional physiological traits phenotyping: new tools to support pre-breeding and plant stress physiology studies. Plant Sci **282**: 49–59

Grassi G, Magnani F (2005) Stomatal, mesophyll conductance and biochemical limitations to photosynthesis as affected by drought and leaf ontogeny in ash and oak trees. Plant Cell Environ **28**: 834–849

Haydon MJ, Mielczarek O, Robertson FC, Hubbard KE, Webb AAR (2013) Photosynthetic entrainment of the Arabidopsis thaliana circadian clock. Nature **502**: 689–692

Hermida-Carrera C, Kapralov M V., Galmés J (2016) Rubisco catalytic properties and temperature response in crops. Plant Physiol **171**: 2549–2561

Hetherington AM, Woodward FI (2003) The role of stomata in sensing and driving environmental change. Nature **424**: 901–908

Janssens SB, Vandelook F, De Langhe E, Verstraete B, Smets E, Vandenhouwe I, Swennen R (2016) Evolutionary dynamics and biogeography of Musaceae reveal a correlation between the diversification of the banana family and the geological and climatic history of Southeast Asia. New Phytol **210**: 1453–1465

Jones HG (1998) Stomatal control of photosynthesis and transpiration. J Exp Bot **49**: 387–398

Jones HG (1985) Partitioning stomatal and non-stomatal limitations to photosynthesis. Plant Cell Environ **8**: 95–104

Kaiser E, Morales A, Harbinson J, Heuvelink E, Prinzenberg AE, Marcelis LFM (2016) Metabolic and diffusional limitations of photosynthesis in fluctuating irradiance in Arabidopsis thaliana. Sci Rep **6**: 1–13

Kimura H, Hashimoto-Sugimoto M, Iba K, Terashima I, Yamori W (2020) Improved stomatal opening enhances photosynthetic rate and biomass production in fluctuating light. J Exp Bot **71**: 2339–2350

Lawson T, Blatt MR (2014) Stomatal size, speed, and responsiveness impact on photosynthesis and water use efficiency. Plant Physiol **164**: 1556–1570

Lawson T, Morison JIL (2004) Stomatal function and physiology. The Evolution of Plant Physiology. Elsevier, Amsterdam, Netherlands, pp 217–242

Lobo FDA, de Barros MP, Dalmagro HJ, Dalmolin ÂC, Pereira WE, de Souza ÉC, Vourlitis GL, Rodríguez Ortíz CE (2013) Fitting net photosynthetic light-response curves with Microsoft Excel – a critical look at the models. Photosynthetica **51**: 445–456

Matthews JSA, Vialet-Chabrand SRM, Lawson T (2017) Diurnal variation in gas exchange: the balance between carbon fixation and water loss. Plant Physiol **174**: 614–623

McAusland L, Vialet-Chabrand S, Davey P, Baker NR, Brendel O, Lawson T (2016) Effects of kinetics of light-induced stomatal responses on photosynthesis and water-use efficiency. New Phytol **211**: 1209–1220

Mencuccini M, Mambelli S, Comstock J (2000) Stomatal responsiveness to leaf water status in common bean (Phaseolus vulgaris L.) is a function of time of day. Plant Cell Environ **23**: 1109–1118

Morales A, Kaiser E (2020) Photosynthetic acclimation to fluctuating irradiance in plants. Front Plant Sci **11**: 1–12

Mott KA, Woodrow IE (2000) Modelling the role of Rubisco activase in limiting non-steady-state photosynthesis. J Exp Bot **51**: 399–406

Outlaw WHJ (2003) Integration of cellular and physiological functions of guard cells. CRC Crit Rev Plant Sci **22**: 503–529

Paine CET, Marthews TR, Vogt DR, Purves D, Rees M, Hector A, Turnbull LA (2012) How to fit nonlinear plant growth models and calculate growth rates: an update for ecologists. Methods Ecol Evol **3**: 245–256

Papanatsiou M, Petersen J, Henderson L, Wang Y, Christie JM, Blatt MR (2019) Optogenetic manipulation of stomatal kinetics improves carbon assimilation,water use, and growth. Science **363**: 1456–1459

Pearcy RW (1990) Sunflecks and photosynthesis in plant canopies. Annu Rev Plant Physiol Plant Mol Biol **41**: 421–453

Perrier X, De Langhe E, Donohue M, Lentfer C, Vrydaghs L, Bakry F, Carreel F, Hippolyte I, Horry JP, Jenny C, et al. (2011) Multidisciplinary perspectives on banana (Musa spp.) domestication. Proc Natl Acad Sci USA **108**: 11311–11318

Prioul JL, Chartier P (1977) Partitioning of transfer and carboxylation components of intracellular resistance to photosynthetic CO2 fixation: a critical analysis of the methods used. Ann Bot **41**: 789–800

Qu M, Hamdani S, Li W, Wang S, Tang J, Chen Z, Song Q, Li M, Zhao H, Chang T, et al. (2016) Rapid stomatal response to fluctuating light: an under-explored mechanism to improve drought tolerance in rice. Funct Plant Biol **43**: 727

Raven JA (2014) Speedy small stomata? J Exp Bot **65**: 1415–1424

Resco de Dios V, Gessler A (2018) Circadian regulation of photosynthesis and transpiration from genes to ecosystems. Environ Exp Bot **152**: 37–48

Rudall PJ, Chen ED, Cullen E (2017) Evolution and development of monocot stomata. Am J Bot **104**: 1122–1141

Sakoda K, Yamori W, Shimada T, Sugano SS, Hara-Nishimura I, Tanaka Y (2020) Higher stomatal density improves photosynthetic induction and biomass production in Arabidopsis under fluctuating light. Front Plant Sci **11**: 589603

Savitzky A, Golay MJE (1964) Smoothing and differentiation of data by simplified least squares procedures. Anal Chem **36**: 1627–1639

Slattery RA, Walker BJ, Weber APM, Ort DR (2018) The impacts of fluctuating light on crop performance. Plant Physiol **176**: 990–1003

Soleh MA, Tanaka Y, Kim SY, Huber SC, Sakoda K, Shiraiwa T (2017) Identification of large variation in the photosynthetic induction response among 37 soybean [Glycine max (L.) Merr.] genotypes that is not correlated with steady-state photosynthetic capacity. Photosynth Res **131**: 305–315

De Souza AP, Wang Y, Orr DJ, Carmo-Silva E, Long SP (2020) Photosynthesis across African cassava germplasm is limited by Rubisco and mesophyll conductance at steady state, but by stomatal conductance in fluctuating light. New Phytol **225**: 2498–2512

Taylor SH, Long SP (2017) Slow induction of photosynthesis on shade to sun transitions in wheat may cost at least 21% of productivity. Philos Trans R Soc Lond B Biol Sci **372**: 20160543

Turner DW, Thomas DS (1998) Measurements of plant and soil water status and their association with leaf gas exchange in banana (Musa spp.): a laticiferous plant. Sci Hortic **77**: 177–193

Urban O, Šprtová M, Košvancová M, Tomášková I, Lichtenthaler HK, Marek M V. (2008) Comparison of photosynthetic induction and transient limitations during the induction phase in young and mature leaves from three poplar clones. Tree Physiol **28**: 1189–1197

Vialet-Chabrand S, Dreyer E, Brendel O (2013) Performance of a new dynamic model for predicting diurnal time courses of stomatal conductance at the leaf level. Plant Cell Environ **36**: 1529–1546

Vialet-Chabrand SRM, Matthews JSA, McAusland L, Blatt MR, Griffiths H, Lawson T (2017) Temporal dynamics of stomatal behavior: modeling and implications for photosynthesis and water use. Plant Physiol **174**: 603–613

Vico G, Manzoni S, Palmroth S, Katul G (2011) Effects of stomatal delays on the economics of leaf gas exchange under intermittent light regimes. New Phytol **192**: 640–652

Wachendorf M, Küppers M (2017) The effect of initial stomatal opening on the dynamics of biochemical and overall photosynthetic induction. Trees Struct Funct **31**: 981–995

Way DA, Pearcy RW (2012) Sunflecks in trees and forests: from photosynthetic physiology to global change biology. Tree Physiol **32**: 1066–1081

van Wesemael J, Kissel E, Eyland D, Lawson T, Swennen R, Carpentier S (2019) Using growth and transpiration phenotyping under controlled conditions to select water efficient banana genotypes. Front Plant Sci **10**: 1–14

Weyers JDB, Johansen LG (1985) Accurate estimation of stomatal aperture from silicone rubber impressions. New Phytol **101**: 109–115

Wilson KB, Baldocchi DD, Hanson PJ (2000) Quantifying stomatal and non-stomatal limitations to carbon assimilation resulting from leaf aging and drought in mature deciduous tree species. Tree Physiol **20**: 787–797

Yamori W, Kusumi K, Iba K, Terashima I (2020) Increased stomatal conductance induces rapid changes to photosynthetic rate in response to naturally fluctuating light conditions in rice. Plant Cell Environ **43**: 1230–1240